


Monte Carlo Study of Magnetic and Thermal Phase Transitions of a Diluted Magnetic Nanosystem

T. Sahdane¹ · A. Mhirech² · L. Bahmad²  · B. Kabouchi¹

Received: 6 June 2017 / Accepted: 2 August 2017 / Published online: 11 August 2017
© Springer Science+Business Media, LLC 2017

Abstract Monte Carlo (MC) simulation method with the Metropolis algorithm is used to study the magnetic and thermal phase transition properties of a spherical nanoparticle. The system consists of two concentric spheres of rays R_C and R_S , respectively ($R_C < R_S$). For $r < R_C$, the spin is $\sigma = \pm 3/2$ and $\pm 1/2$, and for $R_C < r \leq R_S$, the spin is $S = \pm 7/2$, $+5/2$, $\pm 3/2$, and $\pm 1/2$ with antiferromagnetic interface coupling. Between R_C and R_S , the sites are populated with the probability (p). We present a detailed discussion on the magnetic and thermal phase transition characteristics of the system under consideration. Our investigations show that this system can be used as a magnetic nanostructure possessing potential applications in magnetism.

Keywords Monte Carlo simulation · Magnetic properties · Thermal phase transitions · Compensation temperature · Critical temperature · Diluted system

1 Introduction

Magnetic nanoparticles have attracted much attention in recent decades because of their excellent magnetic properties, and with their small size, the study of the magnetic and thermal characteristics of nanoparticles such as nanosphere, nanotube, and nanocube using several types of methods [1–5] was theoretically and experimentally investigated. Vasilakaki et al. [6] studied in detail the thermal and magnetic transition properties of core/shell antiferromagnetic/ferrimagnetic nanoparticles using the Monte Carlo simulation technique with the Metropolis algorithm. Magnetic phase transitions and hysterical characteristics of a core/shell nanometry based on the MC simulation method have been studied [7–12]. An interesting property in these magnetic systems is the presence of a compensating temperature in which all magnetization is zero at a temperature below the critical temperature [13–16]. This point of compensation at the finite temperature is only found when the near-neighbor interaction between the spin $\sigma = \pm 3/2$ and $\pm 1/2$ and the spin $S = \pm 7/2$, $+5/2$, $\pm 3/2$, and $\pm 1/2$ is taken into consideration. It is pointed out that for appropriate values of the system parameters, the multiple compensation and transition temperatures vary with the change in the particle size value. Wang et al. [17] determined the phase diagram of Ising nanoparticles with cubic structures. Our system consists of two different species of magnetic spin components, the spin σ and the spin S with antiferromagnetic interface coupling (Fig. 1). We perform the MC simulation using the Metropolis algorithm and determine the radius effects of the spherical nanoparticle, probability (p) of impurity, and other system parameters on the phase

✉ L. Bahmad
bahmad@fsr.ac.ma

¹ LaMCSi, Molecular Spectrometry, Optics and Laser Instrumentation Team, Faculty of Sciences Mohammed V University in Rabat, PO Box 1014, Rabat-Agdal, Morocco

² Laboratory of Magnetism and High-Energy Physics (LMPHE-PPR-13), Faculty of Sciences Mohammed V University in Rabat, PO Box 1014, Rabat-Agdal, Morocco

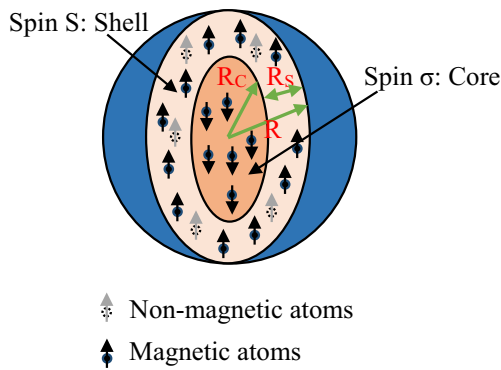


Fig. 1 Schematic representation of the system

transition characteristics of the system under consideration. The outline of this article is as follows: in Section 2, we present our model. The results and discussions are given in Section 3, and, finally, Section 4 contains our conclusions.

2 Model and Monte Carlo Simulation

The system is a core/shell nanoparticle of two concentric spheres of radius R_C and R_S , respectively; we apply free boundary conditions in all directions. The Hamiltonian of the system is given as:

$$H = -J_C \sum_{ij} \sigma_i \sigma_j - J_S \sum_{ij} \varepsilon_i \varepsilon_j S_i S_j - J_{int} \sum_{ij} \sigma_i \varepsilon_j S_j - H \sum_j (\sigma_j + \varepsilon_j S_j) - \Delta \sum_j \varepsilon_j S_j^2 \quad (1)$$

The interaction between two neighboring atoms belonging to the same zone of radius $r \leq R_C$ or radius $R_C \leq r \leq R_S$ is ferromagnetic whereas the interaction between an atom belonging to the radius zone $r \leq R_C$ and an atom belonging to the radius zone $R_C < r \leq R_S$ is antiferromagnetic.

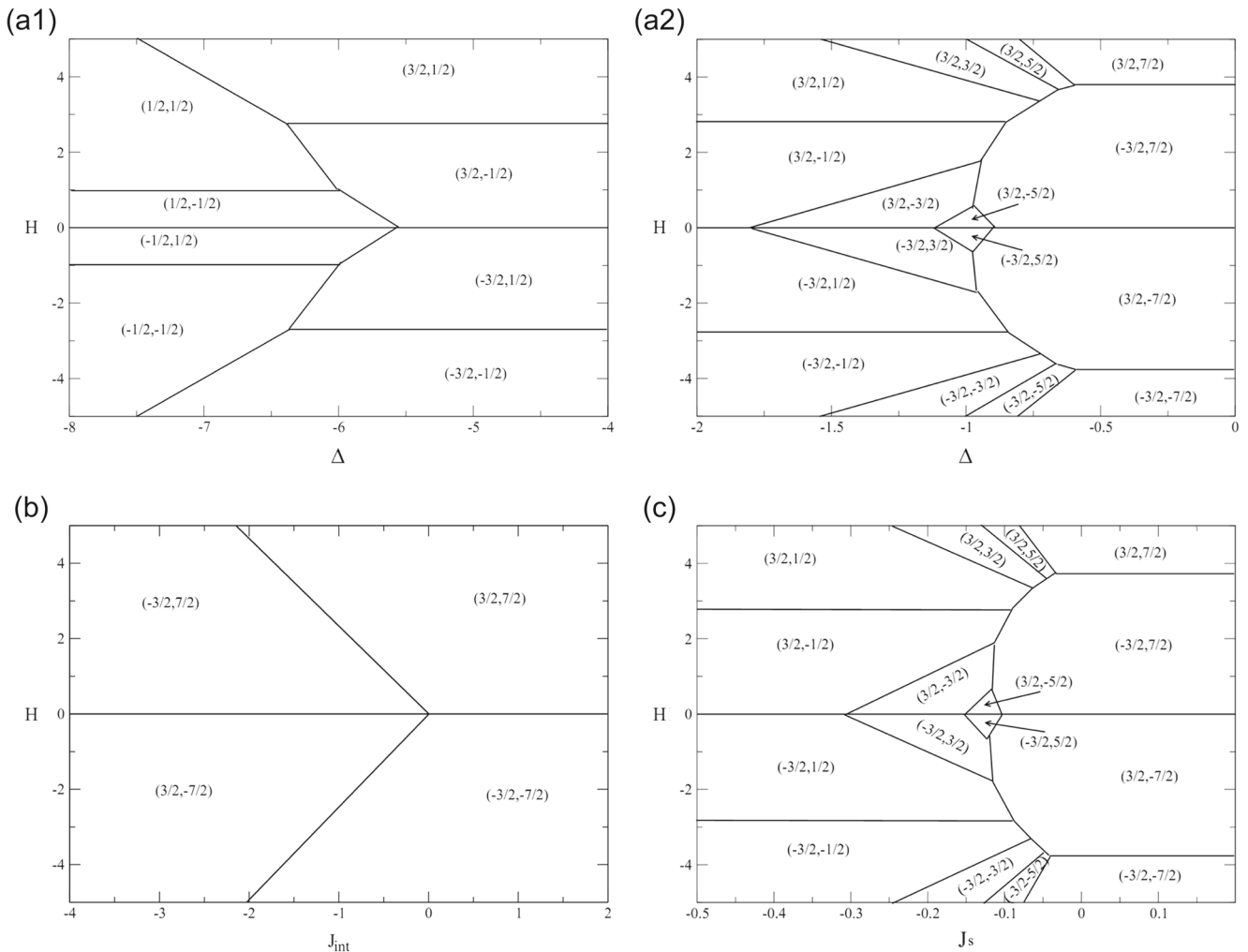


Fig. 2 The ground-state phase diagram: *a* in the plane (Δ, H) , *b* in the plane (J_{int}, H) , and *c* in the plane (J_s, H) ($J_C = 1.0$, $J_S = 0.1$, and $J_{int} = -1.0$)

The radius area $R_C < r \leq R_S$ is randomly diluted with a p to model the presence of a nonmagnetic impurity among S-type atoms. ε_j takes 1 if site j is occupied and take 0 if the site is unoccupied. The J_C , J_S , and J_{int} are the exchange interaction parameters between σ and σ , S and S , and σ and S , respectively. We used the parameter $k_B T / J_C$ where k_B is the Boltzmann constant which is equal to unity. The moment values of the spins are $\sigma = \pm 3/2$ and $\pm 1/2$ and $S = \pm 7/2, \pm 5/2, \pm 3/2$, and $\pm 1/2$. The quantities defined below were calculated using Monte Carlo simulations and used to estimate the critical and compensation temperatures for the model.

Our data were generated with 10^4 Monte Carlo steps per spin. We take a nanoparticle of a core radius $R_C = 6$ and a shell thickness $R_S = 2$; the number of spins in the core is $N_C = 925$, and the number of spins in the shell is $N_S = p \cdot 1184$ ($N = N_C + N_S = 2109$).

The magnetizations:

$$m_C = \frac{1}{N_C} \sum_i \sigma_i \tag{2}$$

$$m_S = \frac{1}{N_S} \sum_j \varepsilon_j S_j \tag{3}$$

The total magnetization:

$$m_{tot} = \frac{1}{2}(m_C + pm_S) \tag{4}$$

The internal energy per site:

$$E = \frac{\langle H \rangle}{N_C + N_S} \tag{5}$$

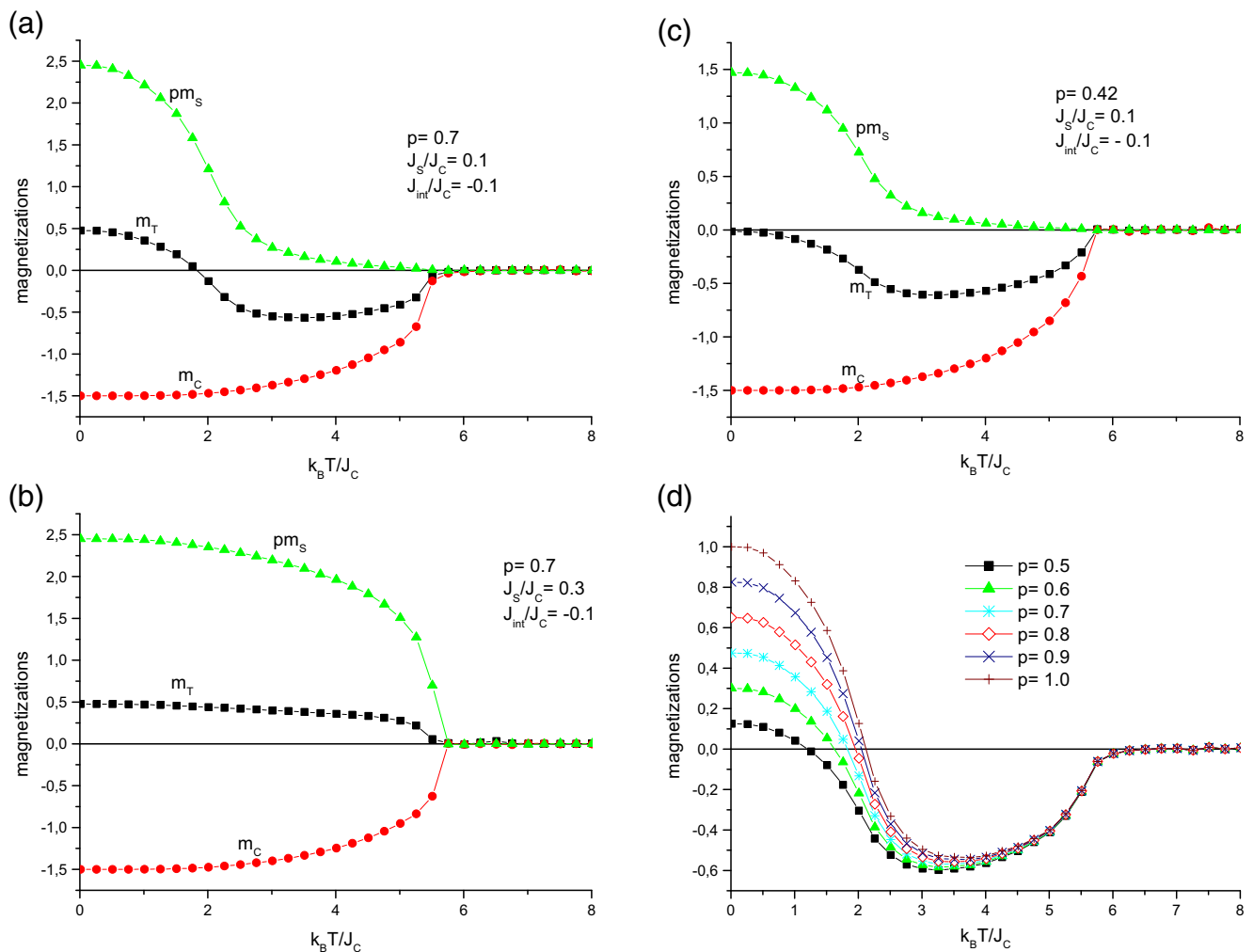


Fig. 3 Core magnetizations (m_C), shell magnetizations (m_S), and total magnetization (m_T) for various temperatures ($k_B T / J_C$) for $p = 0.7$: **a** $J_S / J_C = 0.1$, $J_{int} / J_C = -0.1$, and $\Delta = 0$; **b** for $p = 0.7$: $J_S / J_C = 0.3$,

$J_{int} / J_C = -0.1$, and $\Delta = 0$; and **c** for $p = 0.42$: $J_S / J_C = 0.1$, $J_{int} / J_C = -0.1$, and $\Delta = 0$. **d** Total magnetizations is a function of temperatures: $J_S / J_C = 0.1$, $J_{int} / J_C = -0.1$, and $\Delta = 0$

3 Results and Discussion

Figure 2 (a1, a2) shows the phase diagram of the ground state (Δ , H) which shows the existence of 20 configurations

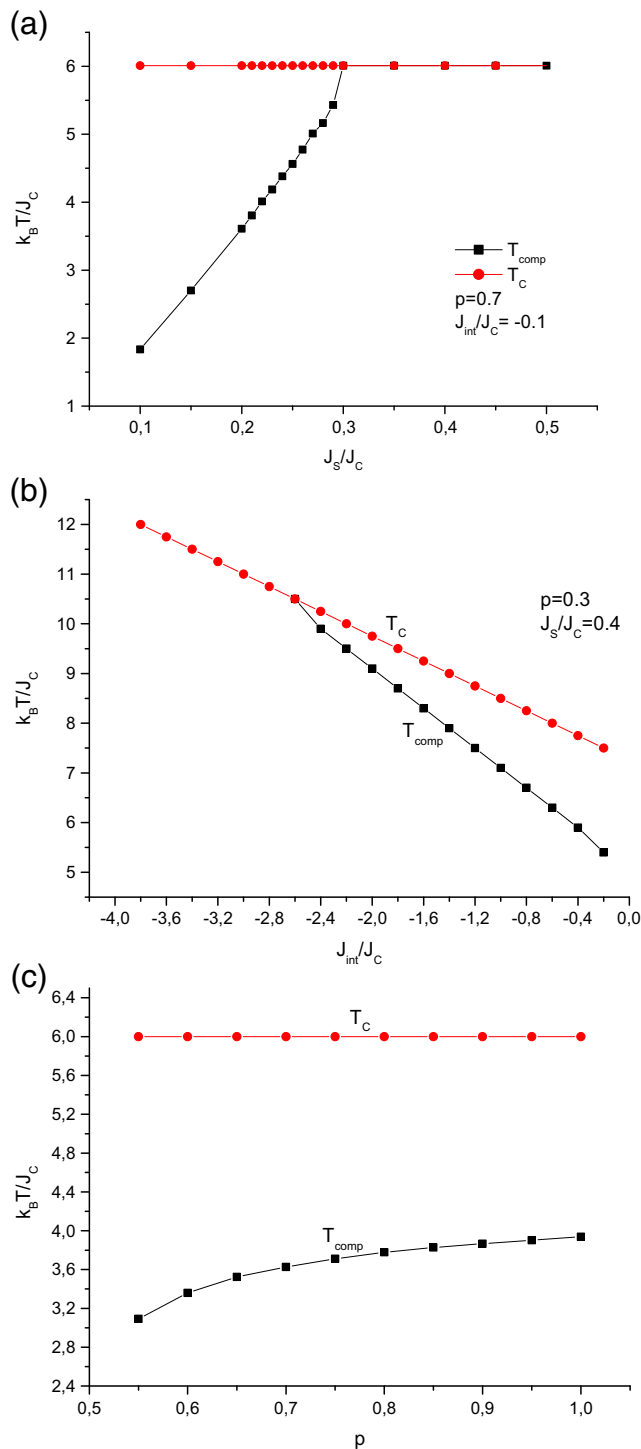


Fig. 4 Critical temperatures (T_C) and compensation temperatures (T_{comp}) is a function probability (p) for **a** $J_S/J_C = 0.7$ and $J_{int}/J_C = -0.1$, **b** $J_{int}/J_C = 0.3$ and $J_S/J_C = 0.4$, and **c** $J_{int}/J_C = -0.1$ and $J_S/J_C = 0.2$

$((-1/2, -1/2), (-3/2, -1/2), (-1/2, 1/2), (-3/2, 1/2), (1/2, -1/2), (3/2, -1/2), (1/2, 1/2), (3/2, 1/2), (-3/2, -3/2), (-3/2, -5/2), (-3/2, -7/2), (-3/2, 3/2), (-3/2, 5/2), (3/2, -7/2), (3/2, 3/2), (3/2, 5/2), (3/2, 7/2), (3/2, -3/2), (3/2, -5/2), (-3/2, 7/2))$, which are stable.

The phase diagram of the ground state (J_{int} , H) shows the existence of four configurations $((-3/2, 7/2), (3/2, 7/2), (3/2, -7/2), (-3/2, -7/2))$, which are stable for $J_{int} < 0$ and $H > 0$; $J_{int} > -2$ and $H > 0$; $J_{int} < 0$ and $H < 0$; and $J_{int} > -2$ and $H < 0$, respectively (Fig. 2 (b)).

Figure 2 (c) illustrates the phase diagram of the ground state (J_S , H) which shows the existence of 16 configurations $((-3/2, -1/2), (-3/2, 1/2), (3/2, -1/2), (3/2, 1/2), (-3/2, -3/2), (-3/2, -5/2), (-3/2, -7/2), (-3/2, 3/2), (-3/2, 5/2), (3/2, -7/2), (3/2, 3/2), (3/2, 5/2), (3/2, 7/2), (3/2, -3/2), (3/2, -5/2), (-3/2, 7/2))$, which are stable.

Figure 3a presents the total magnetization with respect to the reduced temperature $k_B T/J_C$; it can be seen that the

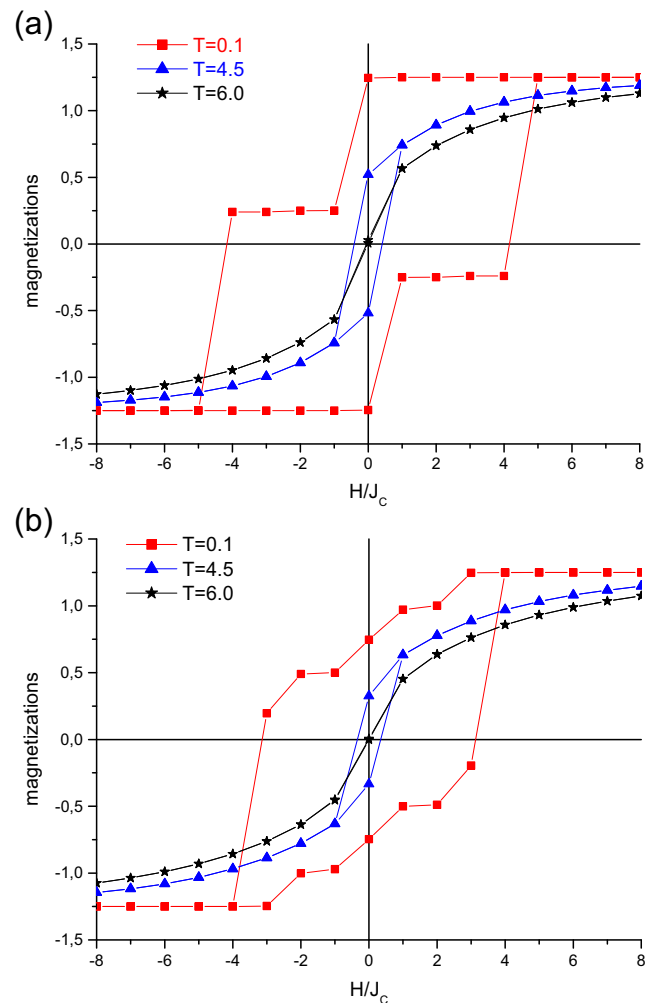


Fig. 5 Magnetic hysteresis cycle for different values of temperatures for **a** $p = 0.7$, $J_S/J_C = 0.1$, $J_{int}/J_C = -0.1$, and $\Delta = 0$ and **b** $p = 0.7$, $J_S/J_C = 0.1$, $J_{int}/J_C = -0.1$, and $\Delta = -1.0$

magnetization curves have two zeros. The first corresponds to the temperature value at which the total magnetization (m_T) reduces to zero, while the subnetworks m_C and m_S are different from zero; it corresponds to the compensation temperature (T_{comp}). The second zero indicates the temperature at which the m_T , m_C , and m_S magnetizations decrease to zero; it corresponds to the critical temperature of the system Curie temperature (T_C). For $p = 0.7$, $J_S/J_C = 0.1$ and $J_{\text{int}}/J_C = -0.1$ show a T_{comp} such that $m_T = 0$ and $0 < T_{\text{comp}} < T_C$. Figure 3b shows that for $p = 0.7$, $J_S/J_C = 0.3$ and $J_{\text{int}}/J_C = -0.1$ show no compensation effect. Figure 3c shows that for $p = 0.42$, $J_S/J_C = 0.1$ and $J_{\text{int}}/J_C = -0.1$ shows no compensation effect. Figure 3d presents that the total magnetization is a function of temperatures for different probabilities ($J_S/J_C = 0.1$, $J_{\text{int}}/J_C = -0.1$, and $\Delta = 0$).

In order to study the influence of J_S/J_C on both critical and system compensation temperatures, the phase diagram is plotted in Fig. 4a, in the plane (T , J_S/J_C). It may be noted that as the value of J_S/J_C increases, the T_C remains constant; for compensation, it exists only when J_S/J_C is less than 0.3 and increases linearly with J_S/J_C .

In the plane (T , J_{int}/J_C), the absolute value $|J_{\text{int}}/J_C|$ increases and the T_C increases; for compensation, it exists only when $|J_{\text{int}}/J_C|$ is less than 2.6 and increases linearly with $|J_{\text{int}}/J_C|$ (Fig. 4b).

The T_C remains constant, and the temperature compensation increases slightly with the p (Fig. 4c).

Figure 5a, b shows that the region of the magnetic hysteresis cycle decreases with increasing temperature and disappears completely for $T = 6.0$

4 Conclusions

In this work, we used the Monte Carlo simulation using the Metropolis algorithm to study the phase diagrams and the thermal and magnetic properties of a diluted system.

We studied the influences of interactions between crystal fields, interfacial interaction, and exchange interaction on critical behaviors and system compensation for a spherical nanoparticle. It can be seen that, depending on the set of Hamiltonian parameters, we can have different types of topologies of phase diagrams with many interesting phenomena. As regards the compensation temperature, we have shown that it exists only within a certain range of system parameters; this range depends closely on the Hamiltonian parameters.

References

1. El Mir, L., Ben Ayadi, Z., Saadoun, M., Von Bardeleben, H.J., Djessas, K., Zeinert, A.: Phys. Status Solidi A. **204**, 3266–3277 (2007)
2. Choi, E.J., Ahn, Y., Hahn, E.J.: J. Korean Chem. Soc. **53**, 2090–2094 (2008)
3. Anil Kumar, P., Mitra, S., Mandal, K.: Indian J. Pure Appl. Phys. **45**, 21–26 (2007)
4. Chiriac, H., Moga, A.E., Gherasim, C.: J. Optoelectron. Adv. Mater. **10**, 3492–3496 (2008)
5. Mhirech, A., Aouini, S., Alaoui-Ismaili, A., et al.: J. Supercond. Nov. Magn. **30**, 925 (2017). doi:10.1007/s10948-016-3867-6
6. Vasilakaki, M., Trohidou, K.N., Nogués, J.: Sci. Rep. **5**, 9609 (2015)
7. Stanley, H.E.: Phase transitions and critical phenomena, p. 9. Clarendon, Oxford (1971)
8. Dias, R.A., Rapini, M., Costa, B.V.: Braz. J. Phys. **36**(3b), 1074–1077 (2006)
9. Vasil'ev, A.N., Bozhko, A.D., Khovailo, V.V., Dikshtein, I.E.: Phys. Rev. B. **59**, 1113 (1999)
10. Zhang, X., Novotny, M.A.: Braz. J. Phys. **36**(3a), 664–671 (2006)
11. Li, S., de La Cruz, C., Huang, Q., Chen, Y.: Phys. Rev. B. **79**, 054503 (2009)
12. Endoh, Y., Matsuda, M., Yamada, K., Kakurai, K.: Phys. Rev. B. **40**, 7023 (1989)
13. Bahmad, L., Benyoussef, A., El Kenz.: Physica A: Stat. Mech. Appl. **387**, 825–833 (2008)
14. Zaim, A., Kerouad, M., Amraoui, Y.E.: J. Magn. Magn. Mater. **321**, 1077–1083 (2009)
15. Buendia, G.M., Cardona, R.: Phys. Rev. B. **59**, 6784 (1999)
16. Nakamura, Y.: Phys. Rev. B. **62**, 11742 (2000)
17. Wang, H., Zhou, Y., Lin, D.L., Wang, C.: Phys. Status Solidi B. **232**, 254–263 (2002)